Supplementary Information

Investigating Li Microstructure Formation on Li Anodes for Lithium Batteries by *In Situ* ^{6}Li/^{7}Li NMR and SEM

Hee Jung Chang,[a] *Nicole M. Trease,*[a,d] *Andrew J. Ilott,*[b] *Dongli Zeng,*[c] *Lin-Shu Du,*[a]

Alexej Jerschow[b] *and Clare P. Grey**[a,d]

[a] Department of Chemistry, Stony Brook University, Stony Brook, New York, 11794-3400, United States.

[b] Department of Chemistry, New York University, 100 Washington Square East, New York, New York, 10003, United States.

[c] Chemistry Department, Brookhaven National Laboratory, Upton, New York, 11793-5000, United States.

[d] Department of Chemistry, University of Cambridge, Lensfield Road, Cambridge, CB2 1EW, United Kingdom

E-mail: cpg27@cam.ac.uk

Susceptibility Calculations Methodology

Following methodology recently implemented by some of the current authors[1], susceptibility calculations were used to understand how the growth of microstructure on the surface of the Li electrodes impacts the Li NMR spectrum. These calculations were performed using the FFT (fast Fourier transform) method described in Refs [2] and [3], whereby the resulting magnetic field maps can be calculated from arbitrary distributions of magnetic spins. The input configuration is specified as a regularly spaced 3D grid of magnetic susceptibilities representing the underlying model. The result of the calculation is a susceptibility-corrected field map at each point on the calculation grid, H_{eff}, which alone would account for a distribution of chemical shifts at different positions in the cell. However, the chemical shifts in the experimental spectra of ^{7}Li inside the conductor are also affected by the Knight shift, caused by the paramagnetic, conducting electrons in the metal. This is accounted for in the calculation results by adding a constant offset, K, to the field results, $H_{exp} = (1 + K) H_{eff}$, where K = 0.0261% for ^{7}Li metal.[4, 5] We note that this offset is reported as K = 0.0263 % for ^{6}Li,[5] but this small difference will not affect the universality of the conclusions drawn from the calculations, which are all done using K for ^{7}Li. Representations of the NMR spectra were made from the H_{exp} maps by creating a histogram of the shifts for the voxels of interest, adding artificial Lorentzian line broadening of 5 ppm to aid the comparison with the experimental spectra.

An array of 512^3 points was used for the input grid, representing a cubic cell with 12.775 mm sides, making each point in the array correspond to a 25 μm^3 voxel; of the order of the microstructure size and the effective skin depth of the Li metal. A single Li electrode was represented by a cuboid in the center of the cell measuring 4.0 × 10.0 × 0.4 mm in the x, y, z directions, with $\mathbf{B_0}$ aligned along z, matching the geometry of the NMR experiments. Voxels

inside the cuboid were assigned a volume susceptibility of $\chi_{Li} = 24.1 \times 10^{-6}$ in SI units[6, 7], with the rest of the cell modeled as a vacuum with $\chi = 0.0$.

The formation of microstructure on the electrode was modeled by randomly assigning voxels next to the surface of the major face of the electrode (the 4.0 × 10.0 mm, xy face) as Li metal (i.e. setting $\chi = \chi_{Li}$ in those voxels) and repeating the calculation. This configuration is illustrated in the inset of Figure 8 in the main text, where the voxels highlighted in pink correspond to the microstructure. Two effects were investigated: (i) the changes in the spectrum of the microstructure as it was increased from a single voxel in length (a mossy microstructure, Figure 8a) to 8 voxels in length (a dendritic microstructure, see also the inset of Figure 8b), and (ii) the changes in the ^{7}Li spectrum of the metal making up the original surface layer as the surface coverage increased (Figure 3a).

In situ NMR acquisition

The full series of *in situ* ^{7}Li nuclear magnetic resonance (NMR) spectra acquired in real time as a symmetric Li metal cell with 1M $LiPF_6$ in EC/DMC (ethylene carbonate/ dimethyl carbonate, 1:1 by vol.) was charged is shown in Figure S1. The cell was charged by a applying a constant current of 1.1 mA/ cm^2 for a total of 240 min as spectra were continuously acquired, with each spectrum taking 2 min to acquire.

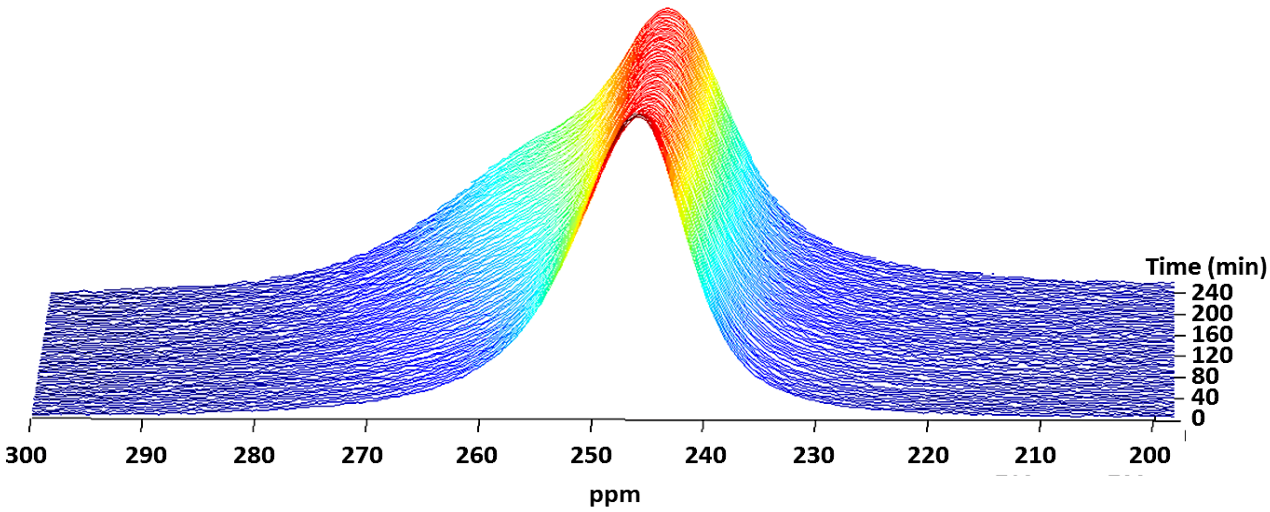

Figure S1. Stacked plot of *in situ* ^{7}Li static NMR spectra of a symmetrical lithium cell with Celgard separator containing $LiPF_6$ in EC/ DMC (1:1 by vol) obtained at 1.1mA/cm^2 as a function of time. The intensity is normalized to the signal at t = 0 min.

Deconvolutions of the NMR Spectra

The deconvolution of NMR spectra was performed by a least-square fitting of the recorded lineshapes in 3 different ways (Figure S2) in order to explore the sensitivity of the relative intensities to the method used to deconvolute the spectra. The NMR signal within the range of 245 to 280 ppm was fit with a combination of Gaussian/Lorentzian lineshapes and the change in

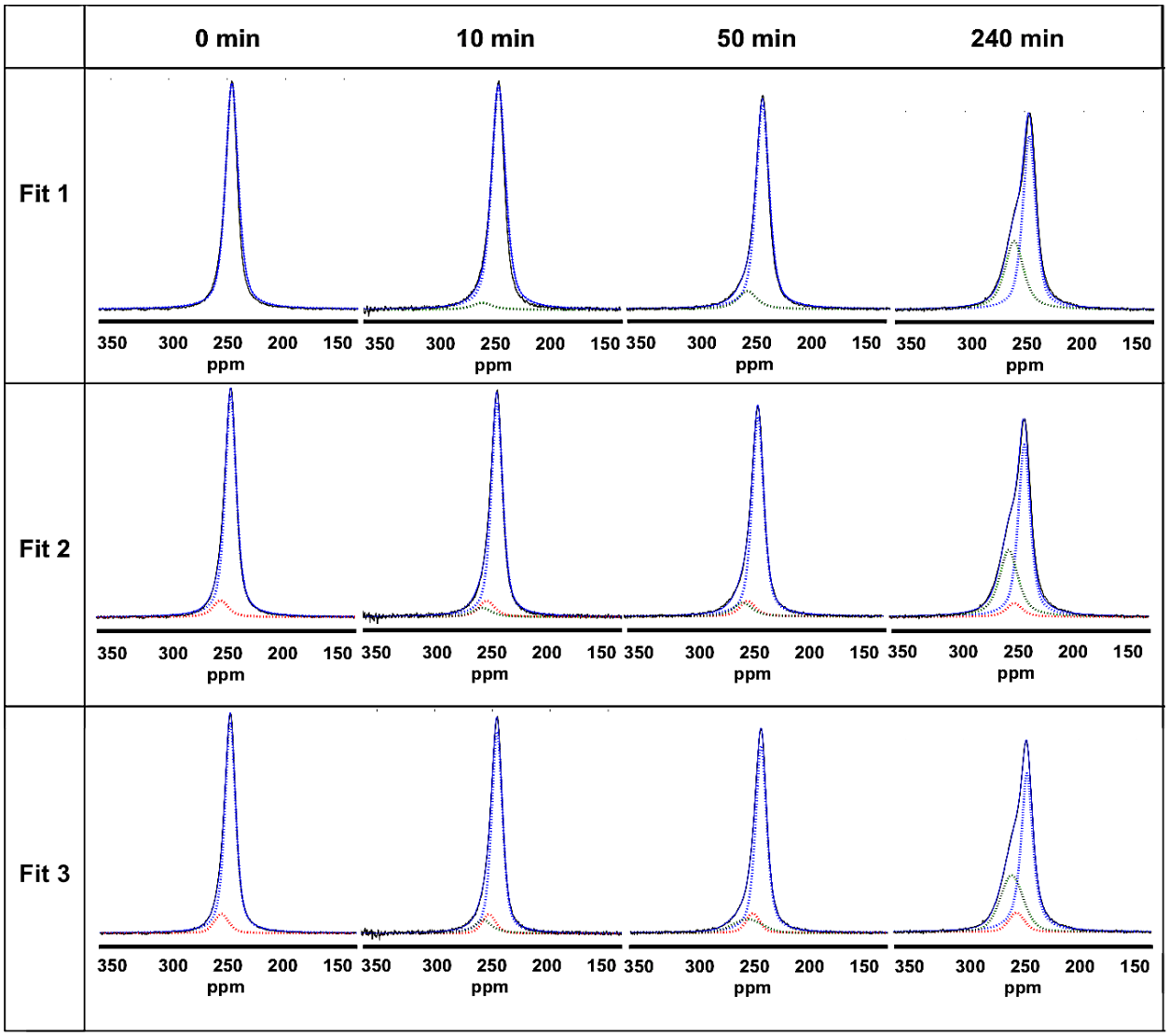

Figure S2. Deconvoluted ^{7}Li static NMR spectra of a symmetrical lithium cell with Celgard separator containing $LiPF_6$ in EC/ DMC (1:1 by vol) obtained at 1.1mA/cm^2 for 0 min, 10 min, 50 min, and 240 min. Fit 1 and Fit 2 are performed with constraints on the bulk metal peak, while Fit 3 was performed without constraints. Fit 1 used 1 peak for the bulk Li metal and 1 peak for the microstructures. Fit 2 and Fit 3 used 2 peaks for the bulk Li metal and 1 peak for the microstructures. The fitted peaks are indicated with blue, green and red dotted lines and a thick black and blue line show the experimental spectra and the fit, respectively.

intensity of the bulk metal peak during the *in situ* experiments (i.e., during the formation of Li microstructures) was explored. Fit 1 used a total of 2 peaks, 1 peak for Li bulk metal and 1 peak for Li microstructures. Fit 2 and Fit 3 used a total of 3 peaks, 2 peaks for Li bulk metal and 1

peak for Li microstructures. The addition of a second peak to fit the Li bulk metal is consistent with our earlier work[8] and is ascribed to the different shift from the minor faces of the Li metal strips that are parallel to $\mathbf{B}_0$ (the bulk of the signal comes from the major faces perpendicular to $\mathbf{B}_0$). For each of the different fitting procedures, the fit parameters (amplitude, position, FWHM (full width at half maximum) and the ratio of the Gaussian/Lorentzian (G/L) line shape) were initially optimized on the spectra at t = 0 min for the bulk metal peak(s) and at t = 240 min for the microstructure peak, and were then used as the initial values for fitting all the *in situ* spectra. Since the shape of the bulk metal could be expected not to change during cycling, constraints were imposed on the fits. In Fit 1 and 2, the parameters were constrained to the initial values for each spectrum, except for amplitude. In Fit 1, only the amplitude of peaks was allowed to vary. For Fit 2, the ratio of the intensity (integrated area) of the 2 bulk metal peaks (blue and red dotted lines) was held constant to account for the intensity of the bulk metal peak decreasing as a function of time. In Fit 2, the peak positions and FWHM were allowed to vary by ±0.5 ppm, and the G/L ratio was constrained between 0.3 and 0.4. In Fit 3 strict constraints were not imposed on the fit parameters, only the peak positions of the 3 peaks were constrained to ensure a 3 peak fit (bulk metal 1: 245 to 246.5 ppm; bulk metal 2: 252 to 254 ppm; microstructure: 258 to 260 ppm).

A decrease in the integrated area of the bulk metal peak was observed in all fitting results. Under the freedom from constraints, Fit 3 shows that the reduction in peak amplitude results from peak broadening, which increased by 7%. The results from these fits are shown in Table S1.

Peak Fits		Fit 1		Fit 2			Fit 3		
Spectra	Fit Parameters	Bulk	Micro	Bulk	Bulk 2	Micro	Bulk	Bulk 2	Micro
0 min	Amp. (arb. units)	1		0.98	0.07		0.97	0.09	
	Pos. (ppm)	246.1		246.1	254.8		246.1	254.0	
	FWHM (ppm)	13.0		11.3	15.8		11.2	15.1	
	G/L	0.40		0.35	0.35		0.38	0.60	
	Area (arb. units)	17.78		15.40	1.62		14.98	1.69	
10 min	Amp. (arb. units)	0.97	0.03	0.94	0.07	0.04	0.92	0.09	0.04
	Pos. (ppm)	246.1	259.8	246.1	254.8	259.8	246.1	253.1	259.0
	FWHM (ppm)	13.0	18.8	11.3	15.8	18.8	11.0	14.0	17.60
	G/L	0.40	0.30	0.40	0.40	0.40	0.48	0.60	0.00
	Area (arb. units)	17.26	0.79	14.59	1.53	1.01	13.50	1.56	1.74
50 min	Amp. (arb. units)	0.88	0.08	0.88	0.07	0.06	0.84	0.09	0.06
	Pos. (ppm)	246.1	259.8	246.1	254.8	259.8	246.0	253.2	259.0
	FWHM (ppm)	13.0	18.8	11.3	15.8	18.8	11.5	14.0	31.1
	G/L	0.40	0.30	0.40	0.35	0.30	0.38	0.6	0.99
	Area (arb. units)	15.69	2.08	14.14	1.49	1.62	13.44	1.56	2.03
240 min	Amp. (arb. units)	0.76	0.30	0.75	0.06	0.29	0.72	0.09	0.26
	Pos. (ppm)	246.1	259.8	245.7	254.2	259.8	245.7	254.0	259.8
	FWHM (ppm)	13.0	18.8	12.0	15.8	18.8	11.9	16.0	23.43
	G/L	0.40	0.30	0.35	0.35	0.30	0.16	0.60	0.70

Table S1. Deconvolution parameters for the ^{7}Li static NMR spectra acquired at different time stages in Figure S1 for Fits 1 – 3. The peak amplitudes (Amp.), peak position (Pos.), FWHM, Gaussian/ Lorentzian ratio (G/L) and integrated area (Area) are given for each fit of the bulk Li metal (Bulk and Bulk 2) and the Li microstructures (Micro). The peak amplitudes in Fit 1 - 3 are normalized by the amplitude of the bulk metal peak in the t = 0 min spectra in Fit 1 to make the changes comparable.

***In situ* ^{7}Li NMR spectra of a Li symmetrical cell during multiple cycling**

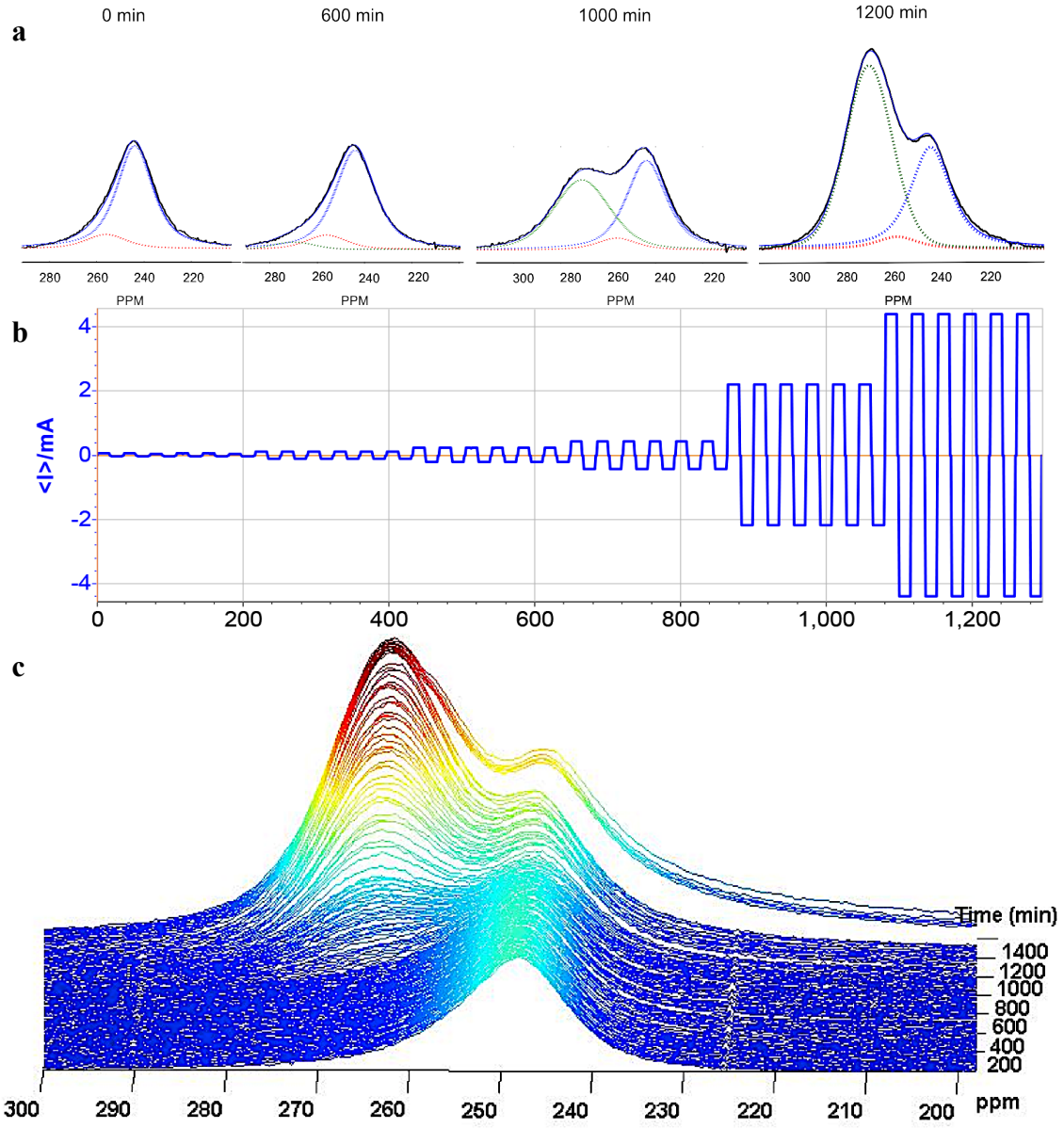

Figure S3. The full *in situ* ^{7}Li NMR spectra of a metallic lithium symmetric cell during multiple cycling with different applied currents. a) Deconvoluted ^{7}Li NMR spectra at four different times (100, 600, 1000, and 1400 min). A total of 3 peaks were used: 2 peaks for Li bulk metal (248 ppm and 258 ppm) and 1 peak for Li microstructures (264 ppm). The deconvoluted peaks are indicated with thin red, blue and green lines and the thick black and blue lines (hidden beneath the black line), shows the experimental the fit spectra, respectively. The normalized intensity of microstructures to bulk metal (sum of blue and red line intensity) each of the spectra is 0.00, 0.05, 0.87, and 1.49 respectively. b) Applied current vs. time with currents of 0.11, 0.275, 0.55, 1.1, 5.5, and 11 mA/cm^2 for multiple cycles. Each cycle consisted of 6 min applied positive current then a 2 min rest followed by 6 min applied negative current and 2 min rest. c) Stacked plot of entire *in situ* ^{7}Li NMR spectra.

***In situ* ^{6}Li and ^{7}Li Data Sets**

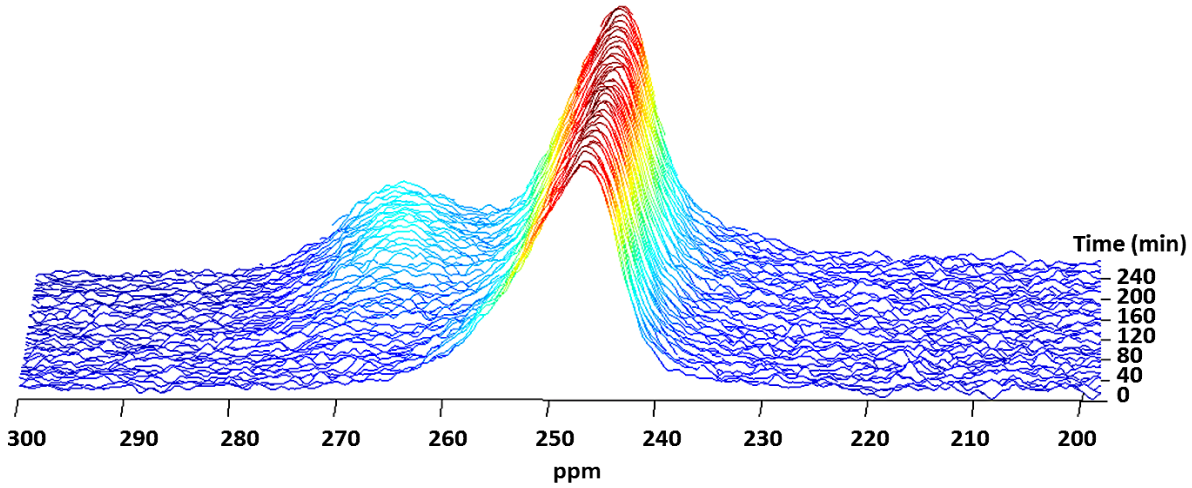

Figure S4. The full *in situ* ^{6}Li NMR spectra of the cell comprised of a ^{6}Li metal strip against ^{7}Li metal with a glass microfiber separator, collected as Li ions move from the ^{6}Li to the ^{7}Li strip at a current of 1.1 mA/cm^{2} for the data in Fig. 5a in the main text.

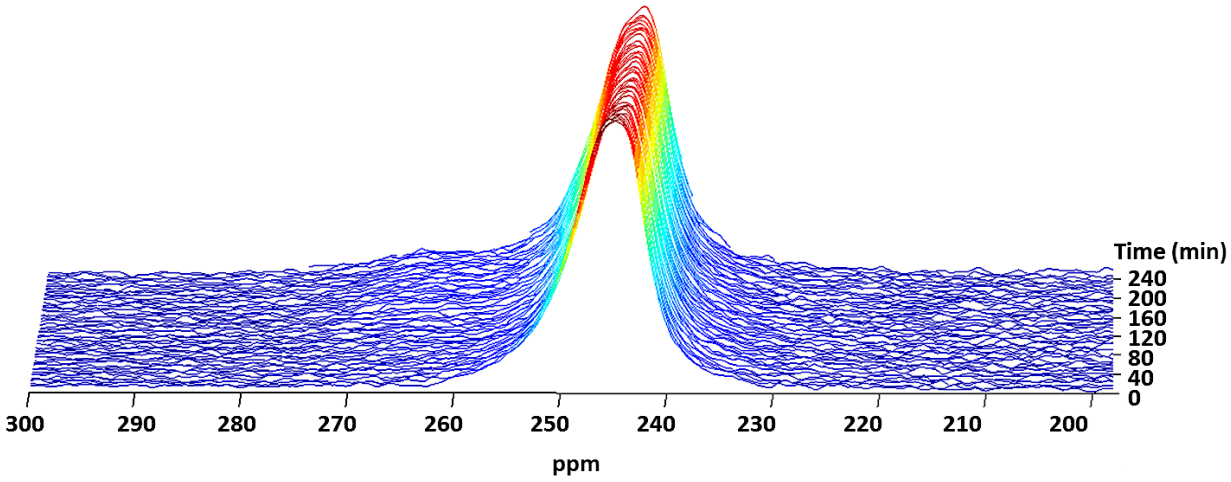

Figure S5. The *in situ* ^{6}Li NMR spectra of the cell comprised of a ^{6}Li metal strip against ^{7}Li metal with a glass microfiber separator, collected as Li ions move from the ^{7}Li to the ^{6}Li strip at a current of 1.1 mA/cm^{2} for the data in Fig. 5b in the main text.

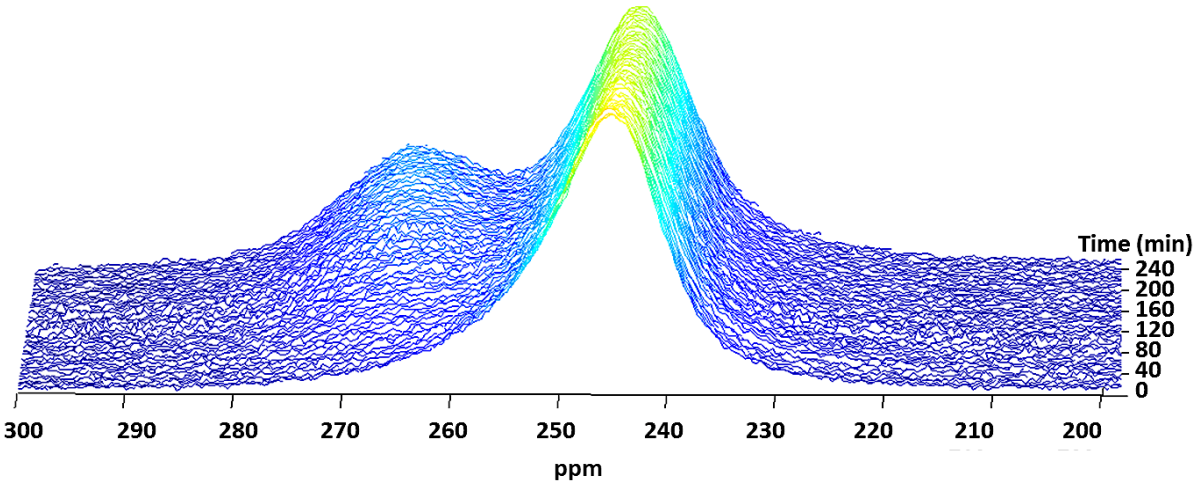

Figure S6. The *in situ* ^{7}Li NMR spectra of the cell comprised of a ^{6}Li metal strip against ^{7}Li metal with a glass microfiber separator collected as Li ions move from the ^{6}Li to the ^{7}Li strip at a current of 1.1 mA/cm^{2} for the data in Fig. 5c in the main text.

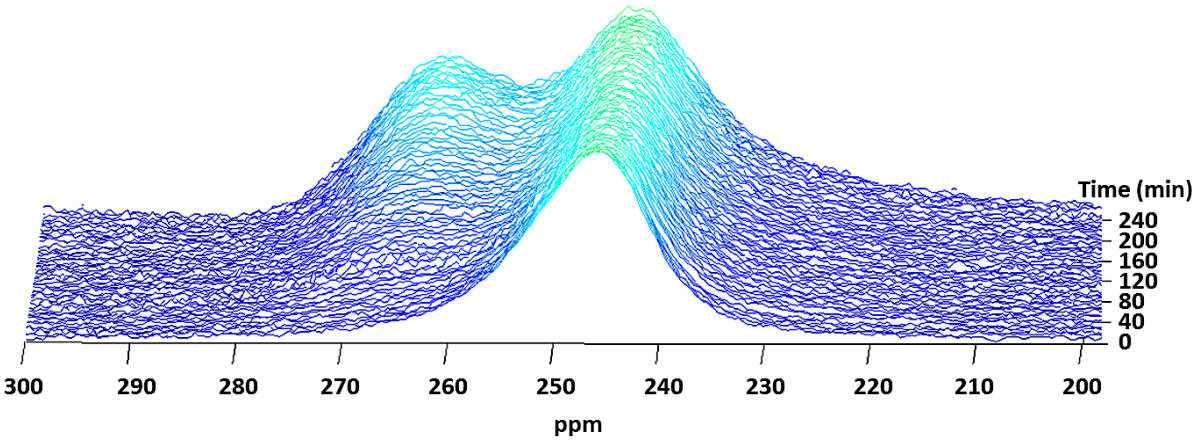

Figure S7. The *in situ* ^{7}Li NMR spectra of the cell comprised of a ^{6}Li metal strip against ^{7}Li metal with a glass microfiber separator collected as Li ions move from the ^{7}Li to the ^{6}Li strip at a current of 1.1 mA/cm^{2} for the data in Fig. 5d in the main text.

References

1. A. J. Ilott, S. Chandrashekar, A. Klöckner, H. J. Chang, N. M. Trease, C. P. Grey, L. Greengard and A. Jerschow, *J. Magn. Reson.*, 2014, **245**, 143-149.
2. R. Salomir, B. D. de Senneville and C. T. W. Moonen, *Concepts Magn. Reson.* , 2003, **19B**, 26-34.
3. J. P. Marques and R. Bowtell, *Concepts Magn. Reson. B* 2005, **25B**, 65-78.
4. H. S. Gutowsky and B. R. McGarvey, *J. Chem. Phys.*, 1952, **20**, 1472-1477.
5. T. J. Rowland, *Prog. Mater Sci.*, 1961, **9**, 3-91.
6. D. Gugan, *Phys. Rev. B*, 1997, **56**.
7. F. T. Hedgcock, *Phys. Rev. Lett.*, 1960, **5**, 420-423.
8. B. Key, R. Bhattacharyya, M. Morcrette, V. Seznec, J. M. Tarascon and C. P. Grey, *J. Am. Chem. Soc.*, 2009, **131**, 9239-9249.